

A COMPREHENSIVE METHODOLOGY FOR EVALUATING SPRINKLER DISCHARGE CHARACTERISTICS

N. Ren, C. Do, and [A. W. Marshall](#)
Department of Fire Protection Engineering
University of Maryland, College Park, MD, USA

Abstract

Water sprays are commonly used in fire suppression applications for cooling the fire environment. This cooling is achieved through the wetting of surfaces (of hot or burning materials) and the evaporation of drops (dispersed in the fire gases) inhibiting both the growth and spread of the fire. The suppression performance of these sprays is determined by their ability to penetrate the fire (i.e. the induced flow) to reach burning surfaces below, while dispersing water throughout the hot environment. Spray penetration and dispersion are governed by the initial drop size and velocity characteristics of the spray, which depend strongly on the injection condition and nozzle configuration. In many fire suppression devices such as sprinklers, a jet is injected onto a deflector to generate the water spray. Although there are many variations on this basic concept, most sprinklers include a central boss surrounded by a deflector having both tines and spaces. In order to study the essential physics of the atomization process, discharge characteristics from a simplified nozzle (having a solid flat deflector without tines or a boss) were measured. These measurements were compared with those from more realistic sprinkler configurations. Flow visualization experiments revealed that the canonical impinging jet configuration produces a smooth radially expanding sheet. While similar atomization mechanisms were observed, realistic sprinkler configurations produce a three-dimensional discontinuous sheet structure with two distinct flow streams corresponding to the tines and spaces of the nozzle. Comprehensive experiments were conducted to describe atomization (e.g. sheet breakup locations, initial drop sizes, and initial velocities) and dispersion (e.g. volume density and local drop size profiles) in these sprays.

Several measurement approaches have been established at the University of Maryland to evaluate the discharge characteristics of the initial spray from sprinklers. In this study, the breakup process responsible for generating the initial spray has been characterized by measuring the trajectories and breakup locations of the radially expanding sheets formed by sprinkler configurations of varying complexity. The trajectories were visualized using a Planar Laser Induced Fluorescence (PLIF) technique. Alternatively, breakup locations were measured using digital short-exposure time flash photography. Novel experiments were also conducted to measure the flow split between the streams deflected along the tines, and the streams created from the flow forced through the spaces. This measurement is important in determining the flow rate and associated thickness of these streams, which has a predominant effect on drop size. For some of the smaller nozzles, drop size was measured 1 m below the sprinkler at several radial locations using a light diffraction based measurement technique. The radial distribution of volume flux was also measured with a mechanical patternator at the same elevation. These measurements provide information about the dispersion behavior from these nozzles. The initial spray has also been characterized with a shadowgraphy technique capable of providing quantitative field measurements of drop size and velocity/flux very close to the nozzle exit. The

first results using this technique on an actual sprinkler (Viking VK102) are provided herein with some experimental details to demonstrate the capabilities of the shadowgraphy method.

The initial drop size and velocity are measured using a *LaVison* shadowgraphy-based direct imaging technique. A dual-cavity NdYag laser is used to produce 30 mJ / pulse of 532 nm light. The beam is directed through a 50 mm diffuser and expanded to approximately 300 mm with a Fresnel lens. A 4 MP digital camera fitted with a 50 mm Canon $f/1.4$ lens is aimed at the illumination field and focused approximately 120 mm in front of the Fresnel lens producing a 150 mm square field of view with a depth of field of approximately 28 mm. The spray is directed in front of the illumination field and through the camera's imaging region partially blocking the light received by the camera and producing distinct shadow images of drops. The pulsed laser and camera are synchronized to provide double images of the drops separated by a short time interval ($\sim 60\mu\text{s}$). A calibration procedure during post-processing provides the drop sizes in each image; while, the drop velocities are determined through comparison of drop trajectories obtained from image pairs and the image pair separation time. Two hundred image pairs were obtained providing tens of thousands of drop sizes and velocities at a given imaging station (i.e. $150 \times 150 \times 28$ mm imaging region). The sprinkler is traversed and rotated to sweep out a large hemispherical interrogation region (from multiple imaging stations) extending radially between approximately 100 mm and 400 mm.

The shadowgraphy technique provides insight into the initial sprinkler spray with unprecedented detail. **Figure 1** shows drop size and velocity data from a Viking VK102 sprinkler operating at 1.4 bar, highlighting a portion of the spray hemisphere extending radially from 150 to 350 mm. The measurements aligned with the tines are indicated in (red, pink) and the measurements aligned with the spaces are indicated in (blue, cyan). To facilitate visualization of general spray patterns, the data has been repeated about the nozzle axis assuming symmetry and ignoring frame arm effects. The tine streams produce very dense sprays concentrated over a narrow elevation angle, ϕ , range; whereas the space streams produce drops distributed over a wide range of elevation angles. It should be noted that both streams produce drops well above the deflector ($\phi < 90^\circ$). Overall spray characteristics are determined by analyzing all drops passing through a fixed radial location corresponding to breakup completion (i.e. spray initiation). The overall drop size distributions and correlation of velocity with drop size are provided in **Figure 2**. The space stream ($\theta < 0^\circ$) produces larger drops than the tine stream ($\theta < 11^\circ$) while drop velocities from both streams are typically much lower than the maximum theoretical velocity ($< 0.8 U_{max}$). The spray hemisphere shown in **Figure 1** reveals spatial distributions in mass flux and drop size, which are quantified in **Figure 3**. Large azimuthal variations in mass flux, but only slight variations in drop size are observed at the peak tine mass flux location ($r = 325$ mm, $\phi = 100^\circ$). Large variations in mass flux and drop size are observed in the elevation profiles with smaller drops typically occurring above the deflector ($\phi < 90^\circ$) in the tine stream and directly below the deflector ($\phi > 150^\circ$) for the space stream. The radial profiles of spray measurements aligned with the space and tine and averaged over all ϕ show that the breakup process continues up to about 325 mm for the tine stream and about 175 mm for the space stream where the drop size begins to stabilize (anomalous behavior noted in the last 2 space stream data points).

Advanced measurements of sprinkler discharge, especially by quantitative shadowgraphy, provides invaluable data for characterizing sprinkler discharge. These detailed measurements can be used to support the development of complex sprinkler injectors, atomization model development, and spray specification for CFD simulations.

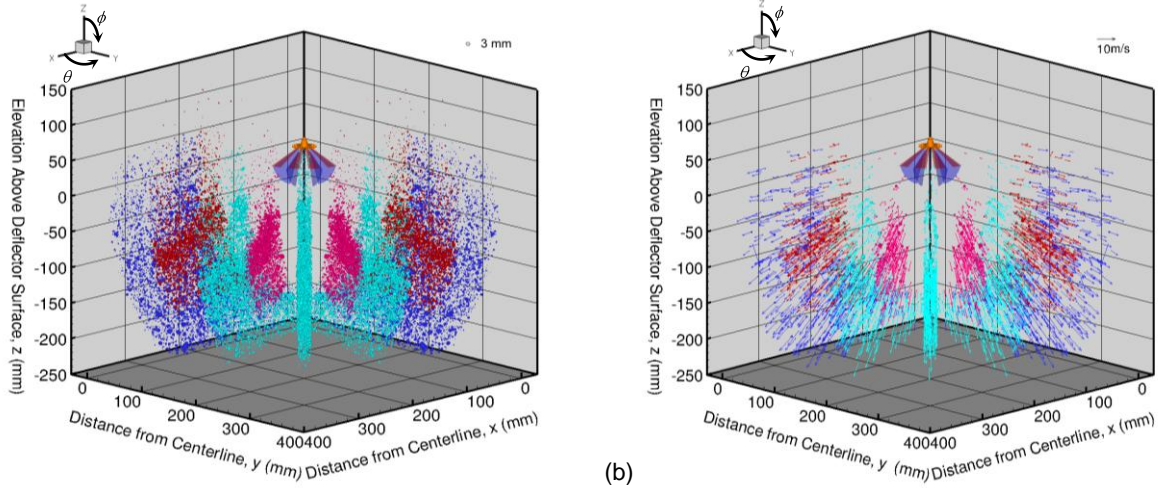


Figure 1: Sprinkler measurements of the near-field spray hemisphere; (a) drop size field; (b) velocity field.

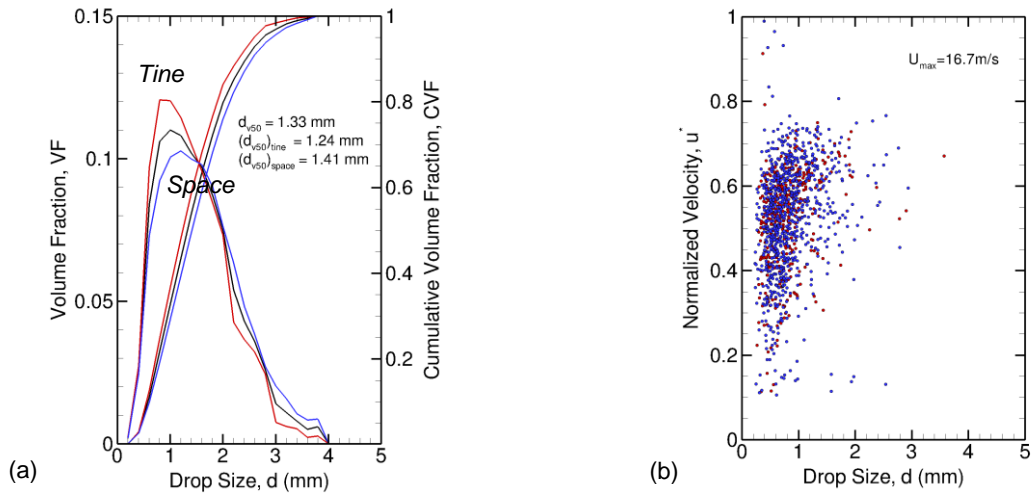


Figure 2: Overall spray characteristics (a) Drop size distribution; (b) Correlation of velocity and drop size.

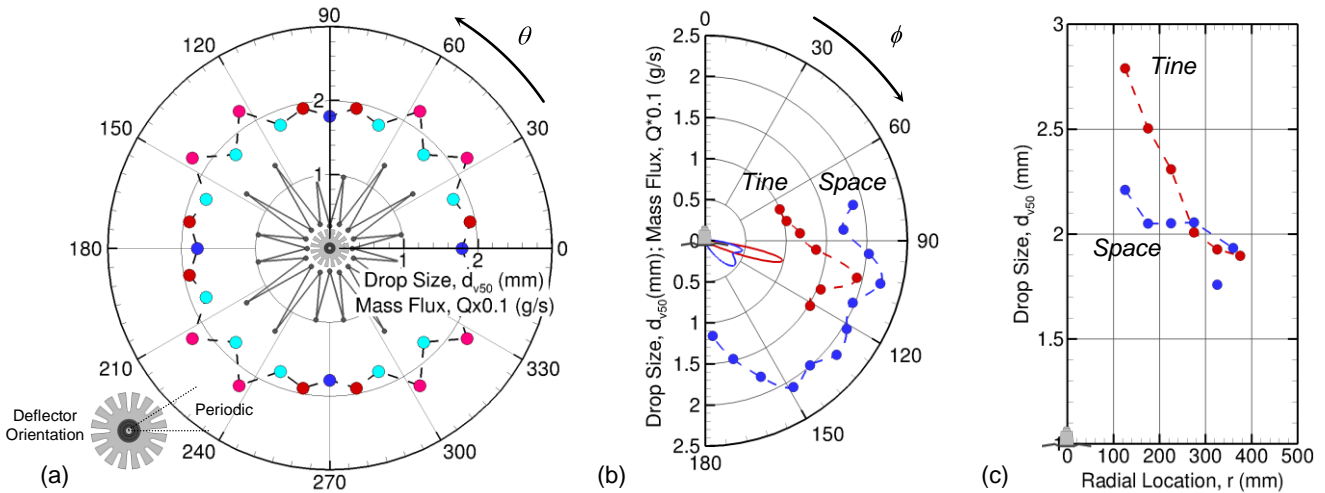


Figure 3: Near field spatial distribution of drop size, mass flux (solid lines) and drop size (circles); (a) mass flux and drop size azimuthal profiles at ($r = 325$ mm, $\phi = 100^\circ$); (b) mass flux and drop size elevation profiles at ($r = 275$ mm, $\theta = 0^\circ$ - space) and ($r = 325$ mm, $\theta = 11^\circ$ - tine); (c) drop size radial profiles at ($\theta = 0^\circ$, all ϕ - space) and ($\theta = 11^\circ$, all ϕ - tine).